Surface Rearrangement of Diblock Copolymer Brushes—Stimuli Responsive Films

William J. Brittain[1] (✉) · Stephen G. Boyes[1,2] · Anthony M. Granville[1] ·
Marina Baum[1] · Brian K. Mirous[1] · Bulent Akgun[1] · Bin Zhao[1,3] ·
Carl Blickle[1] · Mark D. Foster[1]

[1]Department of Polymer Science, The University of Akron, Akron, OH 44325-3909, USA
 wjbritt@uakron.edu

[2]Department of Polymer Science, The University of Southern Mississippi,
 Hattiesburg, MS 39406, USA

[3]Department of Chemistry, The University of Tennessee, Knoxville, TN 37996, USA

Abstract This article reviews results from our group of the synthesis and characterization of diblock copolymer brushes. Results from the literature are also covered. We report a wide variety of diblock compositions and compare the miscibility of the two blocks with the tendency to rearrange in response to block-selective solvents. Also, we describe the types of polymerization methods that can be utilized to prepare diblock copolymer brushes. We have compared the molecular weight of free polymer and the polymer brush based on results from our laboratory and other research groups; we have concluded that the molecular weight of the free polymer and that of degrafted polymer brushes is similar.

Keywords ATRP · Block copolymers · Polymer brushes · Stimuli-responsive · Thin films

Abbreviations

ATRP	atom transfer radical polymerization
RAFT	reversible addition fragmentation transfer polymerization
PS	polystyrene

PMMA   poly(methyl methacrylate)
PMA   poly(methyl acrylate)
PDMA   poly(N,N-dimethylacrylamide)
SAM   self-assembled monolayer
PDMAEMA   poly((N,N'-dimethylamino)ethyl methacrylate)
RATRP   reverse atom transfer radical polymerization
PAA   poly(acrylic acid)
PFS   poly(pentafluorostyrene)
PHFA   poly(heptadecafluorodecyl acrylate)
PTFA   poly(trifluoroethyl acrylate)
XPS   X-ray photoelectron spectroscopy
ATR-FTIR   attenuated total reflectance Fourier transform infrared spectroscopy
TGA   thermal gravimetric analysis
PDI   polydispersity index
AFM   atomic force microscopy

1
Introduction

Polymer brushes refer to an assembly of polymer chains which are tethered by one end to a surface or interface [1, 2]. Tethering of the chains in close proximity to each other forces the chains to stretch away from the surface to avoid overlapping. Polymer brushes are typically synthesized by two different methods, physisorption and covalent attachment. Of these methods, covalent attachment is preferred as it overcomes the disadvantages of physisorption which include thermal and solvolytic instabilities [3, 4]. Covalent attachment of polymer brushes can be achieved by either "grafting to" or "grafting from" techniques. The grafting-to technique involves tethering preformed end-functionalized polymer chains to a suitable substrate [5]. This technique often leads to low grafting density and low film thickness, as the polymer molecules must diffuse through the existing polymer film to reach the reactive sites on the surface. The steric hindrance for surface attachment increases as the tethered polymer film thickness increases. To overcome this problem, the grafting-from approach can be used and has generally become the most attractive way to prepare thick, covalently tethered polymer brushes with a high grafting density [3]. The grafting-from technique involves the immobilizing of initiators onto the substrate followed by in situ surface-initiated polymerization to generate the tethered polymer brush. Surface immobilized initiators are usually generated using self-assembled monolayer (SAM) techniques [6, 7]. As the chains are growing from the surface, the only limit to propagation is diffusion of monomer to the chain ends, thus resulting in thick tethered polymer brushes with high grafting density.

The field of stimuli-responsive films has grown enormously in the past few years. This review will principally concentrate on work from the primary

author's research, but it is obligatory and responsible to highlight some of the recent advances in other research groups. While not comprehensive, this succinct overview will help the reader in the identification of important and relevant research in other groups.

Recent advances in polymer synthesis techniques have given rise to the importance of controlled/"living" free radical polymerization, as it provides a number of advantages over traditional free radical techniques [8]. Although other polymerization methods have been used, one of the main advantages controlled/living free radical polymerization provides for polymer brush synthesis is control over the brush thickness, via control of molecular weight and narrow polydispersities [9, 10]. Another advantage that a controlled/living free radical system provides is the ability to produce polymer brushes of specific architectures and large range of polymerizable monomers.

Without attempting a bias towards our own work on stimuli-responsive diblock copolymer brushes, the group research of Minko, Stamm, Tsukruk and Luzinov have been equally or more influential in the field of stimuli-responsive films. One important fact to consider throughout any discussion of covalently attached polymer chains is the distinction between chains which exist in the "brush" regime vs. the "mushroom" regime. How this affects stimuli-responsive properties remains an open question; but, for each polymer system, there is clearly a grafting density that defines a transition from the mushroom to brush regime. The reader is referred to a particularly important paper by Genzer and co-workers [11] who clearly defined a grafting density that represented this transition. Although their study only concentrated on polyacrylamide brushes, it serves as a general guide to an approximate grafting density at which an investigator can claim that their covalently attached polymer exists in the brush regime. One clear assertion that can be drawn from the literature is that any grafted polymer prepared by the grafting-to technique will inevitably lead to a covalently attached system in the mushroom regime which will be characterized by low film thicknesses.

Stimuli-responsive surface polymers are typically characterized by either binary systems (two chemically dissimilar chains attached to the same surface) or homopolymer brushes based on poly(acrylamide) [especially poly(N-isopropyl)acrylamide, pNIPAA] which demonstrate temperature-dependent conformational changes. Desai and co-workers [12] performed ATRP of N-isopropyl acrylamide (NIPAA) onto oxidized films of oxidized polypropylene and observed stimuli-responsive behavior. Scanning-probe lithography was used by Zauscher et al. [13, 14] to create a patterned array of ATRP initiators for the preparation of nanopatterned pNIPAA polymer chains that demonstrated reversible height changes via a transition cycling of the substrate between water and water/methanol mixtures. Grafting-from of NIPAA from polystyrene latex particles was reported by Kizhakkedathu and co-workers [15]; the hydrodynamic thickness of the latex particles was

controlled by the polymerization conditions and block copolymers with *N,N*-dimethylacrylamide were also reported. Farhan and Huck [16] reported the formation of pNIPAA layers on oxidized polyester films; in addition, they created patterned thermoresponsive films using microcontact printing. One interesting report was the use of pH to control film behavior in a modified copolymer of NIPAA and glycinylacrylamide [17]. Zhu et al. [17] observed typical polyelectrolyte brush behavior above pH 8.0 but the film thickness decreased substantially at lower pH values (5.0) presumably due to hydrogen-bonding between glycine side chains. Using a Si(100) (Si – H) surface for a grafting-to method, Xu and co-workers [18] studied the cell attachment of the cell line 3T3 Swiss albino on both homopolymers of pNIPAA and poly(ethylene glycol) monomethacrylate (PEGMA). Above the lower critical solution temperature (LCST) of pNIPAA, the cells proliferated but below the LCST, cells detached spontaneously. The PEGMA surface was very effective at preventing cell attachment and growth. However, incorporation of PEGMA units into the pNIPAA chains via copolymerization resulted in a more rapid cell detachment during the LCST transition. This work represents an inter-esting example of a stimuli-responsive surface for the controlled adhesion of cells. Somewhat related to the work on pNIPAA brushes is work from the group of Ito and co-workers [19] where they have studied the permea-bility of membranes modified with poly(acrylic acid) as a function of pH. Although Ryan and co-workers [20] did not focus on homopolymer brushes, they studied innovative multiblock systems composed of a hydrophobic end-block and either polyacid or polybase mid-block; this comprehensive study used a battery of techniques to follow molecular shape change and macro-scopic deformation.

There have been a number of reports on binary brushes which refer to a mixture of two different polymer chains attached to the same surface. Zhao and co-workers [21, 22] have reported some novel systems using a surface im-mobilized dual initiator which clearly produces polymer brushes. Their work will be discussed later in this review. An extensive body of work has been pub-lished on binary systems using predominately grafting-to methods; many of these reports have provided provocative results on stimuli-responsive poly-mer systems. Minko, Stamm and co-workers [23] demonstrated a reversible patterning of a stimuli-responsive film based on a binary brush composed of poly(2-vinylpyridine) (PVP) and polyisoprene. Exposure to different sol-vents demonstrated a switching behavior; furthermore, crosslinking of the polyisoprene by illumination through masks created a patterned surface that showed location-dependent stimuli-responsive behavior. In related work, switchable binary brushes were prepared on silicon wafers composed of PVP and a polystyrene copolymer containing a photodimerizing phenylindene component [24]. Water contact angle changes of 40 degrees were observed depending on the polarity of the solvent to which the sample was exposed. The structural state of the switchable surface could be fixed by photoinduced

crosslinking of the phenylindene unit. In subsequent work, the same principle authors developed an "anchoring layer" to prepare binary brushes [25]. They compared the grafting of polystyrene (PS) and PVP end-grafted chains to either an epoxysilane-modified monolayer or a macromolecular layer composed of poly(glycidyl methacrylate). Sequential deposition of PS and PVP produced binary brushes that differed in wettability and nanomorphology. Minko, Stamm and co-workers [26] fabricated binary films of PS and PVP on polyamide polymer surfaces that had been first treated in an ammonia plasma followed by immobilization of an azo initiator. They observed significant differences in grafting-from a silicon surface and the derivatized polyamide surface. They extended this technique to fabric modification and reported water contact angles up to 150 degrees. Recently, two excellent reviews of the work from Minko and co-workers [27, 28] have been published which details the work described above plus other efforts from their group and their collaborators.

1.1
Block Copolymer Brushes

One of the most interesting of these architectures produced to date are block copolymer brushes. Block copolymer brushes are interesting due to the fact that vertical phase separation results when the block copolymer chains are tethered by one end to a surface or substrate. By changing the grafting density, chain length, relative block length, composition of the blocks or the interaction energy between the blocks and the surrounding environment, the formation of a variety of novel well-ordered structures have been predicted by theory [29, 30] and in some cases demonstrated experimentally [21, 31–34].

2
Synthesis of Block Copolymer Brushes

2.1
Results from Other Research Groups

In this review, synthesis of block copolymer brushes will be limited to the grafting-from method. Hussemann and coworkers [35] were one of the first groups to report copolymer brushes. They prepared the brushes on silicate substrates using surface-initiated TEMPO-mediated radical polymerization. However, the copolymer brushes were not diblock copolymer brushes in a strict definition. The first block was PS, while the second block was a 1 : 1 random copolymer of styrene/MMA. Another early report was that of Matyjaszewski and coworkers [36] who reported the synthesis of poly(styrene-*b*-*tert*-butyl acrylate) brushes by atom transfer radical polymerization (ATRP).

This was the first report using ATRP and sequential monomer addition. Hydrolysis of these diblock copolymer brushes yielded poly(styrene-*b*-acrylic acid) brushes.

During the last 5 years, there have been several reports of multiblock copolymer brushes by the grafting-from method. The most common substrates are gold and silicon oxide layers; but there have been reports of diblock brush formation on clay surfaces [37] and silicon-hydride surfaces [38]. Most of the newer reports have utilized ATRP [34, 38–43] but there have been a couple of reports that utilized anionic polymerization [44, 45]. Zhao and co-workers [21, 22] have used a combination of ATRP and nitroxide-mediated polymerization to prepare mixed poly(methyl methacrylate) (PMMA)/polystyrene (PS) brushes from a difunctional initiator. These Y-shaped brushes could be considered block copolymers that are surface immobilized at the block junction.

2.2
Synthesis of Block Copolymer Brushes in Our Group

The first diblock copolymer brushes synthesized in our group were made by a combination of carbocationic polymerization and ATRP (Scheme 1) [46]. Zhao and co-workers [47] synthesized diblock copolymer brushes consisting of a tethered chlorine-terminated PS block, produced using carbocationic polymerization, on top of which was added a block of either PMMA, poly(methyl acrylate) (PMA) or poly((*N*,*N'*-dimethylamino)ethyl methacrylate) (PDMAEMA), synthesized using ATRP. The thickness of the outer poly(meth)acrylate block was controlled by adding varying amounts of free initiator to the ATRP media. It has been reported that the addition of free initiator is required to provide a sufficiently high concentration of deactivator, which is necessary for controlled polymerizations from the sur-
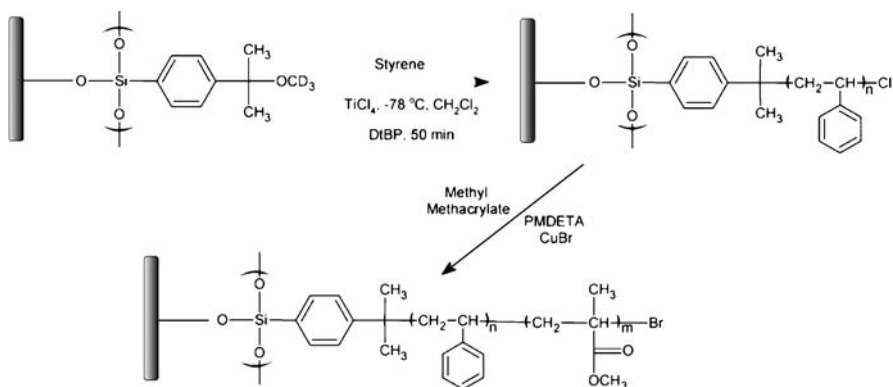
Scheme 1 Synthesis of surface-immobilized diblock copolymer brush (Si/SiO$_2$//PS-*b*-PMMA) using a combination of carbocationic polymerization and ATRP

face [35]. Table 1 summarizes the properties of some of the diblock copolymer brushes.

The first diblock copolymer brush synthesized completely using controlled/living free radical polymerization techniques in our group was by Sedjo and co-workers [48]. In this work a tethered diblock copolymer of PS and PMMA was synthesized using a combination of reverse atom transfer radical polymerization (RATRP) and standard ATRP techniques (Scheme 2). The properties of this diblock copolymer brush can be seen in Table 1. RATRP involves initiation by conventional radical initiators in the presence of an ATRP deactivator. RATRP has been shown to produce polymers that are end-functionalized with a transferable halogen, thus allowing continued polymerization [49, 50]. To perform RATRP from the surface, an azo-initiator was first immobilized on the silicon substrate followed by the polymerization of styrene in the presence of copper(II)bromide and ligand. This resulted in the formation of a tethered block of PS with a terminal bromine group. The terminal bromine group was subsequently used to initiate MMA under standard ATRP conditions.

Table 1 Summary of the properties of diblock copolymer brushes

Diblock copolymer brush structure[a]	Thickness of tethered block [b] (nm)	Thickness of outer block[b] (nm)	Polymerization technique[c]	Refs.
Si/SiO$_2$//PS-b-PMMA	28	11	Cationic/ATRP	[46, 47]
Si/SiO$_2$//PS-b-PMA	24	9	Cationic/ATRP	[47]
Si/SiO$_2$//PS-b-PDMAEMA	27	3	Cationic/ATRP	[47]
Si/SiO$_2$//PS-b-PMMA	25	7	RATRP/ATRP	[48]
Si/SiO$_2$//PS-b-PDMA	11	12	RAFT	[51]
Si/SiO$_2$//PDMA-b-PMMA	11	10	RAFT	[51]
Si/SiO$_2$//PS-b-P(t-BA)	21	17	ATRP	[52]
Si/SiO$_2$//PS-b-PAA	21	8	ATRP/Hydrolysis	[52]
Si/SiO$_2$//PMA-b-P(t-BA)	14	16	ATRP	[52]
Si/SiO$_2$//PMA-b-PAA	14	9	ATRP/Hydrolysis	[52]
Si/SiO$_2$//PS-b-PPFS	16	5	ATRP	[53]
Si/SiO$_2$//PS-b-PHFA	10	6	ATRP	[53]
Si/SiO$_2$//PMA-b-PPFS	11	5	ATRP	[53]
Si/SiO$_2$//PMA-b-PHFA	15	5	ATRP	[53]

[a] PS—polystyrene, PMMA—poly(methyl methacrylate), PMA—poly(methyl acrylate), PDMAEMA—poly((N,N-dimethylamino)ethyl methacrylate), PDMA—poly(dimethylacrylamide), P(t-BA)—poly($tert$-butyl acrylate), PAA—poly(acrylic acid), PPFS—poly(pentafluorostyrene), PHFA—poly(heptadecafluorodecyl acrylate)
[b] Representative structure is Si/SiO$_2$//tethered block-b-outer block
[c] ATRP—atom transfer radical polymerization, RATRP—reverse atom transfer radical polymerization, RAFT—reversible addition fragmentation transfer polymerization
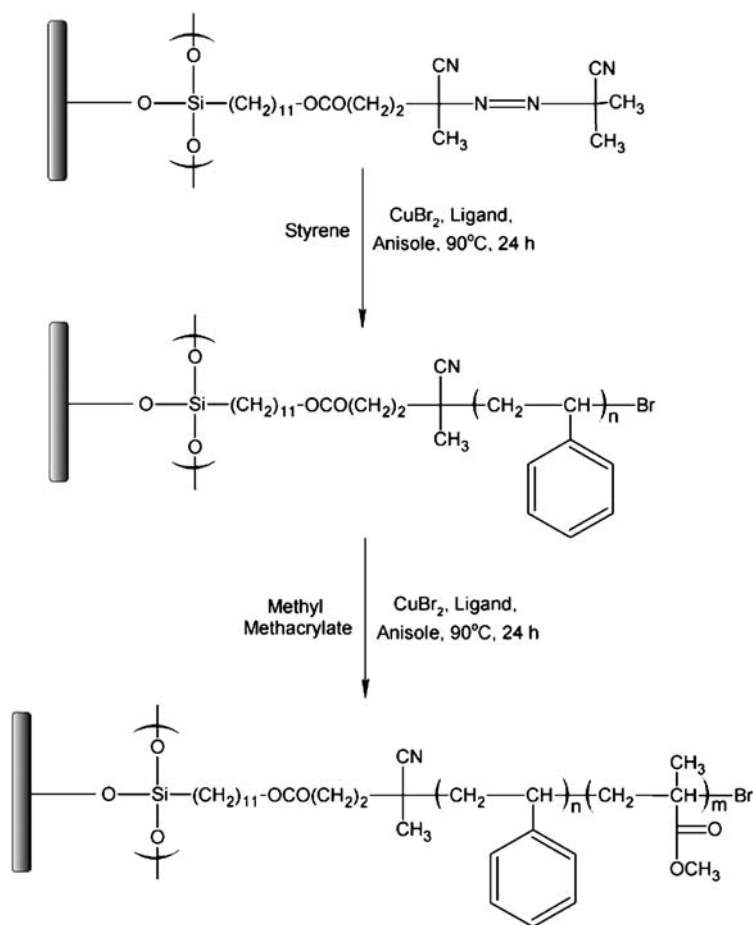
Scheme 2 Synthesis of surface-immobilized diblock copolymer brush (Si/SiO$_2$//PS-*b*-PMMA) using reverse atom transfer radical polymerization and ATRP

To make further use of the azo-initiator, tethered diblock copolymers were prepared using reversible addition fragmentation transfer (RAFT) polymerization. Baum and co-workers [51] were able to make PS diblock copolymer brushes with either PMMA or poly(dimethylacrylamide) (PDMA) from a surface immobilized azo-initiator in the presence of 2-phenylprop-2-yl dithiobenzoate as a chain transfer agent (Scheme 3). The properties of the diblock copolymer brushes produced can be seen in Table 1. The addition of a "free" initiator, 2,2′-azobisisobutyronitrile (AIBN), was required in order to obtain a controlled polymerization and resulted in the formation of free polymer chains in solution.

In order to produce block copolymer brushes by ATRP directly from the surface, the ATRP initiator, (11-(2-bromo-2-methyl)propionyloxy)undecyltri-
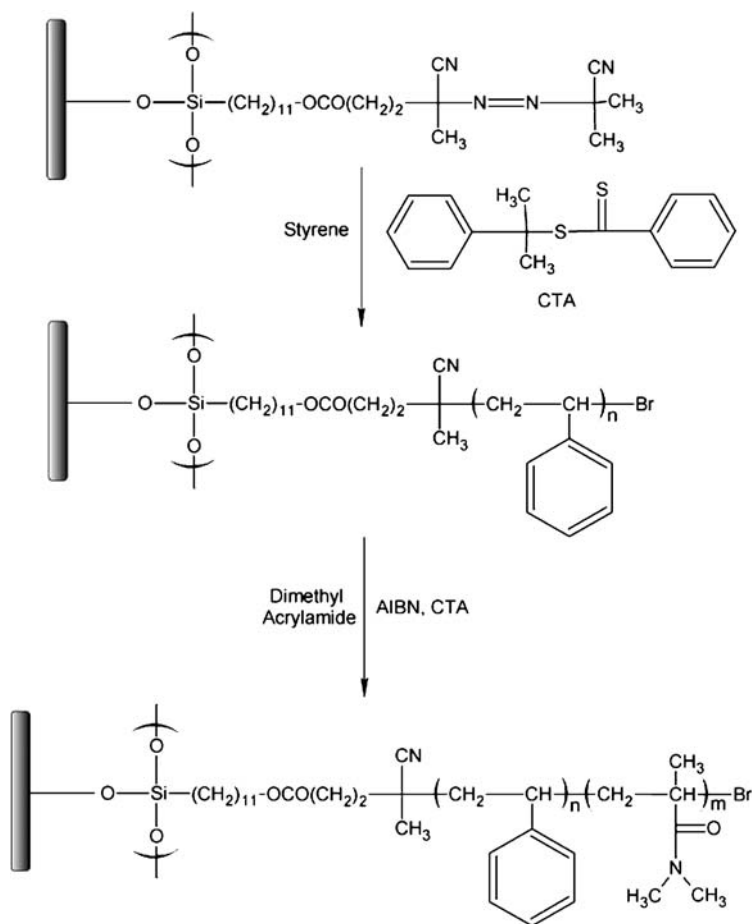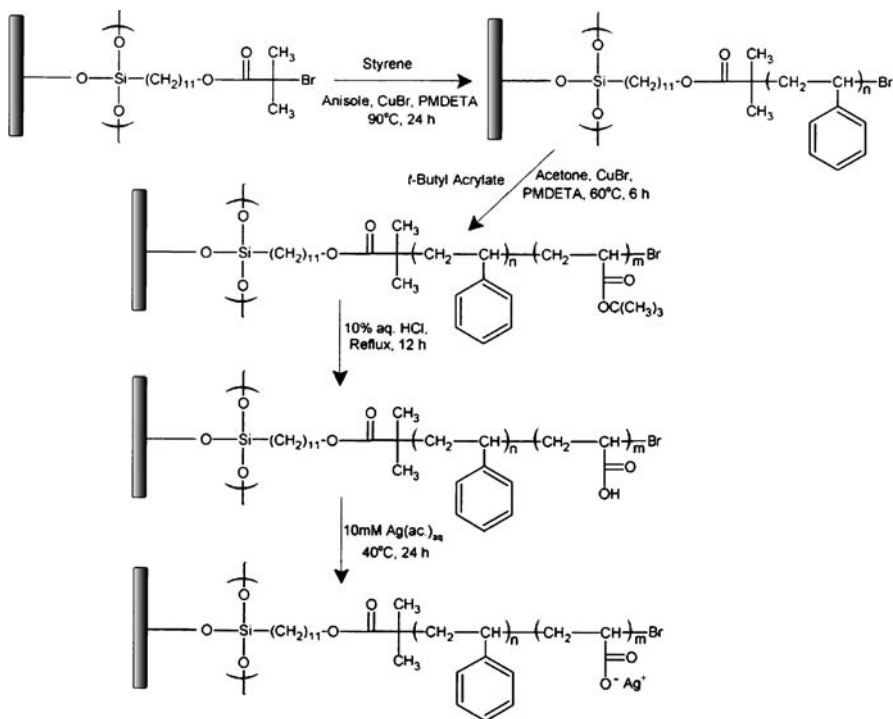
Scheme 3 Synthesis of surface-immobilized diblock copolymer brush (Si/SiO$_2$//PS-*b*-PDMA) using reverse addition fragmentation transfer polymerization

chlorosilane, was prepared and immobilized on silicon substrates. From this immobilized bromo-isobutyrate type ATRP initiator both Boyes and co-workers [52] and Granville and co-workers [53] were able to synthesize diblock copolymer brushes using ATRP. Boyes and co-workers [52] synthesized diblock copolymer brushes of either PS or PMA and poly(*tert*-butyl acrylate) (P(*t*-BA)) using ATRP, with subsequent hydrolysis of the P(*t*-BA) to poly(acrylic acid) (PAA) (Scheme 4). The properties of these diblock copolymer brushes can be seen in Table 1. The diblock copolymer brushes, Si/SiO$_2$//PS-*b*-PAA and Si/SiO$_2$//PMA-*b*-PAA, were both treated with aqueous silver acetate to produce polyelectrolyte diblock copolymer brushes. The polyelectrolyte brushes were subsequently reduced using H$_2$ resulting in the formation of silver nanoparticles within the diblock copoly-

mer brush [52]. Granville and co-workers [53] used similar ATRP techniques to synthesize diblock copolymer brushes that contained the semifluorinated monomers pentafluorostyrene (PFS) and heptadecafluorodecyl acrylate (HFA). The properties of these diblock copolymer brushes can also be seen in Table 1. The use of fluorinated monomers to produce outer blocks of either PPFS or PHFA resulted in surfaces that were highly hydrophobic [53].

We also synthesized a triblock copolymer brush using sequential monomer addition and ATRP. Boyes and co-workers [33] synthesized the ABA type triblock copolymer brushes of PS and PMA to produce $Si/SiO_2//PS$-b-PMA-b-PS and $Si/SiO_2//PMA$-b-PS-b-PMA brushes. We observed incomplete re-initiation for the third block of $Si/SiO_2//PS$-b-PMA-b-PS (as indicated by a 3 nm thickness); the incomplete re-initiation was attributed to radical-radical termination occurring in the formation of the previous blocks. In the case of the $Si/SiO_2//PMA$-b-PS-b-PMA brush, the outer PMA block had a thickness of 15 nm, which is close to the target thickness of 20 nm, indicating that the degree of termination occurring in this system was less.

Scheme 4 Synthesis of surface-immobilized polyelectrolyte diblock copolymer brush ($Si/SiO_2//PS$-b-$PAA(Ag^+)$) using ATRP

3
Correlation of Brush Thickness with Molecular Weight

Before describing the rearrangement of diblock polymer brushes, we will review results from our laboratory and the literature that give a clearer picture of the structure of both homopolymer and copolymer brushes. Specifically, what is known about grafting density and the relationship between brush molecular weight and film thickness. This review focuses on brushes made by either ATRP or RAFT.

Our report [51] on RAFT from surfaces appeared nearly simultaneously with the report of Tsujii and co-workers [54]. Tsujii and co-workers concentrated on a kinetic analysis of PS homopolymer brush formation while we were more interested in using the unique feature of RAFT to polymerize acrylamides. We worked primarily on flat substrates and conducted RAFT by starting with an immobilized azo initiator and running the polymerization in the presence of a RAFT agent and free azo initiator (AIBN). Because free polymer (polymer not covalently bound to the surface) was formed in our RAFT studies, it was possible to compare the molecular weight of free polymer to the degrafted polymer. We used spherical silica particles and immobilized Rühe's initiator [9]. Using thermogravimetric analysis (TGA), we [55] determined that the grafting density was 0.7 initiator molecules/nm^2, a value that corresponds well with Prucker and Rühe [9] (0.8–1.6 initiator molecules/nm^2). We determined the molecular weight for both PMMA and PS brushes. For PMMA, M_n (free polymer) = 15 900 g/mol, PDI = 1.22 and M_n (degrafted polymer) = 19 200 g/mol, PDI = 1.29. For PS, M_n (free polymer) = 10 600 g/mol, PDI = 1.11 and M_n (degrafted polymer) = 11 400 g/mol, PDI = 1.14. There is a close correspondence between both the molecular weight and PDI. The relatively narrow PDI is consistent with a living radical process. Using the molecular weight and TGA data, we determined that the initiator efficiency (f) ranged from 0.15–0.19 [55]. Tsujii and co-workers [54] published a graph comparing molecular weight for degrafted and free PS; inspection suggests that the difference in M_n values was never greater than 4000 g/mol and the PDI for degrafted polymer was slightly higher than free polymer, as we also observed. Patten et al. [56, 57] observed similar trends. The significance of these results is that analysis of free polymer provides a reasonable estimate of the brush molecular weight, thus eliminating the time-consuming chore of performing an analogous procedure on high surface area supports. Knowing the brush molecular weight is important because it allows one to calculate the occupied area of a single polymer brush chain (A_X) using the following equation: $A_X = M_n/(h\rho N_A)$ where ρ = brush bulk density, h = dry brush thickness and N_A is Avogadro's Number. Knowing the relationship between grafting density and solvent-induced rearrangement of diblock copolymer brushes is one of our key objectives.

We have repeated similar degrafting experiments for brush formation via ATRP. While there have been reports on degrafting using conventional radical polymerization [10, 58], this discussion will be limited to brush formation by ATRP. In unpublished work [59], we immobilized an ATRP initiator, (11-(2-bromo-2-methyl)propionyloxy)undecyltrichlorosilane) on Stöber silica and conducted a styrene polymerization. Degrafting of the PS brushes was conducted by etching of the silica cores with HF. From TGA analysis of the immobilized initiator and the corresponding PS brush system, we determined that there are 4.8 initiator molecules/nm^2 and $f = 0.06$. The initiator density corresponds well to the values of 2.4–5.0 reported by Patten and co-workers [56, 57] for the immobilization of (2-(4-chloromethylphenyl)ethyl)dimethylethoxysilane on a similar support.

Brush formation by ATRP can be accompanied by free polymer if the process is conducted with a free initiator. A high concentration of a deactivating Cu(II) complex is necessary for control of ATRP [36]. For ATRP from a surface, the small amount of initiator tethered to the substrate provides too low a concentration of Cu(II) to control the polymerization. One solution to this problem is to add Cu(II) at the beginning of the brush synthesis [36]. Another solution is to use a free initiator, which generates a sufficient Cu(II) concentration in situ. We prefer this latter approach because others and we have observed that the molecular weight of the free polymer roughly corresponds to the molecular weight of the polymer brush. For our PS brush silica gel experiments, [59] we observed M_n (free polymer) = 19 600 g/mol, PDI = 1.11 and M_n (degrafted polymer) = 27 100 g/mol, PDI = 1.57. Von Werne and Patten [56, 57] reported better correspondence for an analogous experiment (ATRP on spherical silica); for PMMA – M_n (free polymer) = 50 700 g/mol, PDI = 1.16 and M_n (degrafted polymer) = 57 100 g/mol, PDI = 1.26; for PS – M_n (free polymer) = 43 800 g/mol, PDI = 1.22 and M_n (degrafted polymer) = 46 300 g/mol, PDI = 1.29. Hawker and co-workers [35] performed nitroxide-mediated radical polymerization of styrene on silica gel; they observed M_n (free polymer) = 48 000 g/mol, PDI = 1.20 and M_n (degrafted polymer) = 51 000 g/mol, PDI = 1.14. In summary, these three studies have demonstrated that there is a reasonable and reliable correlation between the molecular weight and PDI for free polymer and the polymer brush for brush growth via ATRP.

Somewhat related to studies on silica gel is a report by Ejaz and co-workers [60] where they studied the ATRP of MMA on porous glass filters. They examined the relationship between the molecular weight of free polymer and degrafted polymer. While they did not provide the raw data, they presented the results in a graph, which indicates that there was a 35% or less discrepancy between the polymer covalently attached to the frit and that produced by the free initiator. The final literature report that bears notice is that from Kim, Bruening and Baker [61]. To the best of our knowledge of this writer, this is the only report that compared the molecular weight of degrafted

polymer brushes grown on a <u>flat</u> substrate; they used a large gold substrate and degrafted the chains by treatment with I_2. Because they did not use a free initiator, a comparison between free and degrafted polymer was not possible. They observed a nonlinear dependence where the reported M_n of a 33 nm thick film was 33 100 g/mol, while $M_N = 68\,900$ g/mol is observed for a 40 nm thick film. Interestingly, the results of Kim and co-workers match those of Hawker and co-workers [35] at lower molecular weights. One interesting finding in the report by Kim and co-workers is an estimated $f = 0.10$ for ATRP from thiol/gold initiators. This value is reasonably close to the value we observed in our laboratories using ATRP from spherical silica.

In summary, upon review of results from our own laboratories combined with literature results, it is now possible to make reasonable conclusions about the molecular weight and dispersity of polymer brushes. First, it seems that f for living polymerizations approximates 0.10. Second, there is good correspondence between the M_n and PDI of free polymer and degrafted polymer.

4
Rearrangement of Block Copolymer Brushes

The behavior of tethered diblock copolymer brushes is interesting because the bottom block is highly constrained by covalent attachment to the silicate surface and localization of the other end at the diblock interface. Theoretical studies using self-consistent field calculations, scaling arguments and computer simulations have indicated that tethered block copolymer brushes exhibit complex behaviors that depend on many factors [29, 30, 62–65]. These factors include χ, overall molecular weight (N), volume fraction of one block, Kuhn length (flexibility of backbone), grafting density, environmental conditions (solvent, temperature) and the surface free energy of each block in the air. One of the most interesting structures is the "pinned micelle" structure, which can be formed when tethered AB diblock copolymer brushes are treated with a block-selective solvent [29]. To the best of our knowledge, the nomenclature of pinned micelles was originally introduced by Balazs and co-workers [29, 30] and we have adopted this terminology to describe our systems.

4.1
Nanomorphology of Si/SiO$_2$//PS-*b*-PMMA Brush

We reported the synthesis of Si/SiO$_2$//PS-*b*-poly(acrylate) tethered diblock copolymer brushes [31, 32, 46, 47]. The properties of these diblock brushes were studied using water contact angles, ellipsometry, X-ray photoelectron spectroscopy (XPS), FTIR spectroscopy and atomic force microscopy (AFM). For a sample with a 26 nm PS layer and a 9 nm PMMA layer, the advanc-

ing water contact angle increased from 75° (characteristic of PMMA) to 99° (characteristic of polystyrene) after treatment with cyclohexane; subsequent treatment with CH_2Cl_2 returned the contact angle to the original value of 75°. This contact angle change was attributed to reversible changes in the chemical composition at the polymer–air interface. XPS analysis indicated large compositional changes after treatment with CH_2Cl_2 and cyclohexane which are consistent with the contact angle observations.

For a sample with a 23 nm PS layer and 14 nm PMMA layer, AFM was used to study surface morphological changes [32]. It was found the surface is relatively smooth with a roughness of 0.77 nm after CH_2Cl_2 treatment (Fig. 1); treatment with cyclohexane at 35 °C for 1 h increased the surface roughness to 1.79 nm and created an irregular worm-like structure on the surface. A nanopattern was formed if mixed solvents of CH_2Cl_2 and cyclohexane were used and the composition was gradually changed from CH_2Cl_2 to cyclohexane (Fig. 2). The advancing water contact angle of this surface was 120°. We speculated that this nanopattern corresponds to a pinned micelle nanomorphology (Scheme 5), consistent with the theoretical predictions of Balazs and co-workers [29]. Our interpretation of this image as periodic is simply based on a visual inspection; we did not perform Fourier transform analysis to confirm the degree of periodicity.

We explored the relationship between average domain size as deduced by AFM and block lengths for a $Si/SiO_2//PS$-b-PMMA diblock brush [31]. We assumed that the block length is proportional to ellipsometric film thickness. Table 2 contains a summary of the experimental relationship between block lengths (as determined by ellipsometry) vs. average domain diameter for the observed nanomorphologies. For the three samples studied, the largest di-
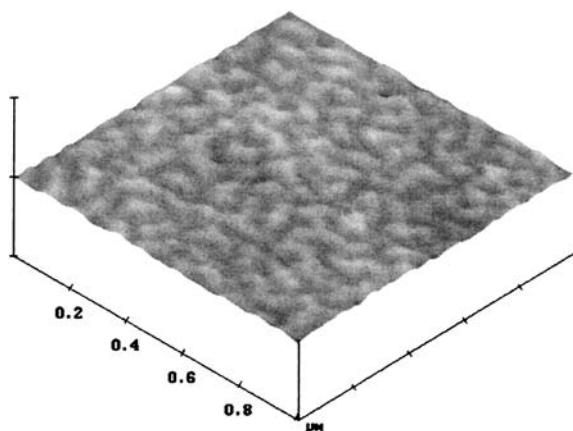

Fig. 1 AFM image of the tethered $Si/SiO_2//PS$-b-PMMA brushes with 23 nm thick PS layer and 14 nm thick PMMA layer after treatment with dichloromethane at room temperature for 30 min and drying with a clean air stream
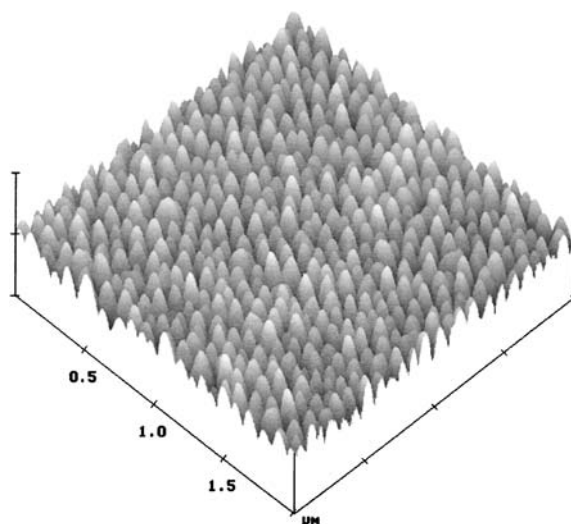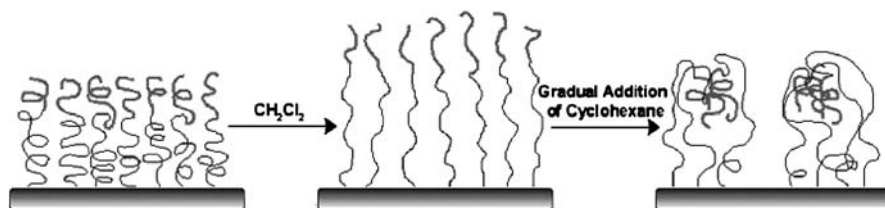
Fig. 2 AFM image of the tethered $Si/SiO_2//PS$-b-PMMA brushes with 23 nm thick PS layer and 14 nm thick PMMA layer after a gradual treatment with cyclohexane

Scheme 5 Speculative model for nanopattern formation from tethered $Si/SiO_2//PS$-b-PMMA

Table 2 Average AFM domain diameter vs. diblock brush thickness [30]

PS Thickness, nm [a]	PMMA Thickness, nm [a]	Domain diameter, nm [b]	Roughness, nm [b]
15	3	46	5.3
23	14	85	13.1
26	17	113	11.7

[a] Thickness determined by ellipsometry
[b] Domain diameter and roughness determined by AFM

block variable is the PMMA thickness. As the thickness of the PMMA layer increases, the average domain diameter of the surface-immobilized micelles also increases. Balazs and co-workers predicted this experimental observa-

tion [29]; self-consistent field theory indicated that pinned micelles should be observed for tethered diblocks where the more soluble block (in our case, PS) is attached to the surface. Furthermore, Balazs and co-workers predicted that the size of the pinned micelles should increase with the size of the less-soluble block (in our case, PMMA), as we have observed.

These intriguing results prompted us to study the effect of different diblock brush compositions on the rearrangement. Although we successfully prepared a series of different diblock brushes and did observe changes in the surface properties (see Sect. 4.2 below), only the $Si/SiO_2//PS$-b-PMMA system displayed a periodic nanomorphology (Fig. 2). The literature contains at least two examples of block brushes that exhibit a similar, periodic nanomorphology in AFM analysis. Zhao and co-workers [21, 22] prepared a well-defined mixed PMMA/PS brush using an asymmetric difunctional initiator-terminated SAM. For mixed brushes where the PS M_n is slightly lower or similar to PMMA M_n, a periodic nanomorphology was observed in the AFM after treatment with acetic acid (a block-selective solvent for PMMA). Huang and co-workers [34] prepared a triblock brush on gold composed of PMMA-b-poly(N,N-dimethylaminoethyl methacrylate)-b-PMMA. A featureless surface was observed for the sample treated with a nonselective solvent (dichloromethane). Methanol was gradually added to the solvent until the composition was 99.5/0.5 (v/v) methanol/dichloromethane; AFM analysis of the triblock revealed a periodic nanomorphology that was attributed to surface-immobilized micelles. We also reported a triblock brush and did observe significant changes in the AFM after treatment with block-selective solvents; however, the observed features were much more disperse (Fig. 3) [33].
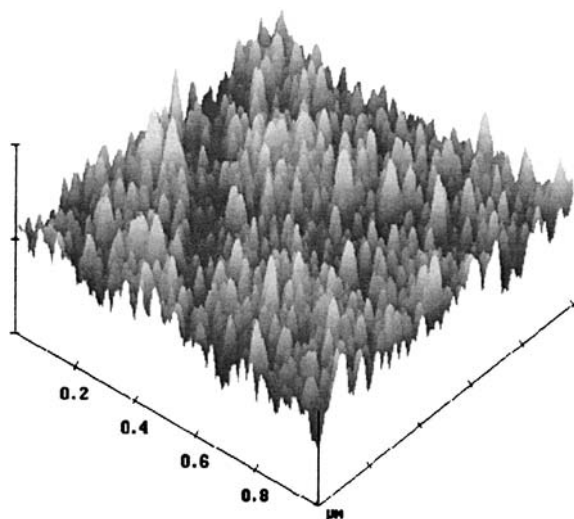

Fig. 3 AFM image of $Si/SiO_2//PMA$-b-PS-b-PMA brushes after treatment with cyclohexane

4.2
Expanded Composition of Diblock Copolymer Brushes

One important goal of this research was to expand the composition of block copolymer brushes. The motivation was to prepare dissimilar (e.g., greater disparity in hydrophobicity) blocks that might show greater changes in the surface properties before and after switching and to use blocks that would respond to nonsolvent induced stimuli (e.g., pH, ionic strength, temperature). We expanded our composition to include the monomers listed in Table 3. Also given in Table 3 are solubility parameters (δ) that were calculated using group contribution methods. The greater the difference in δ, the larger the Flory–Huggins interaction parameter (χ) and thus the less likely that two blocks would be miscible. It is logical to assume that the rearrangement of diblock copolymer brushes would be related to χ; one would predict that the diblocks with the largest χ values would be the least likely to rearrange.

Table 4 contains some representative data for solvent switching of a series of diblock brushes where the bottom block (adjacent to the silicate) is PS. Column 2 of this table contains the advancing, water contact angles for the system in the extended state; that is, the contact angle represents the composition of the upper block. Treatment of the diblock brushes with a PS block-solvent should induce a rearrangement that places PS segments at the air interface; the expected advancing contact angle for a PS-rich surface is

Table 3 Calculated δ based on group contribution methods compared to experimental values [a]

Monomer	Calc. δ $(J/cm^3)^{1/2}$	Exp. δ $(J/cm^3)^{1/2}$
Methyl acrylate (MA)	19.9	19.9–21.3
Methyl methacrylate (MMA)	19.0	18.6–26.2
Styrene (S)	19.1	17.4–19.0
N,N-Dimethylacrylamide (DMA) [b]	25.2	unknown
Acrylic acid (AA) [b]	28.7	unknown
N,N-Dimethylaminoethyl methacrylate (DMAEMA) [b]	19.5	unknown
Hydroxyethyl methacrylate (HEMA) [b]	24.8	unknown
Heptadecafluorodecyl acrylate (HFA)	14.1	unknown
Pentafluoropropyl acrylate (PFA)	16.5	unknown
Trifluorethyl acrylate (TFA)	17.5	unknown
Pentafluorostyrene (PFS)	unknown	16.77 [c]

[a] All values obtained from published work by Van Krevelen or calculated using values of Hoftyzer and Van Krevelen [66]
[b] Values calculated by the method of Fedors [66]
[c] Value obtained from work by Su [67]

Table 4 Solvent induced rearrangement of diblock brushes

Block copolymer brush [a,b]	Starting Θ_a	Θ_a After cyclohexane treatment
Si/SiO$_2$//PS-*b*-PMMA [46] (26) (9)	75	98
Si/SiO$_2$//PS-*b*-PMA [47] (24) (9)	68	98
Si/SiO$_2$//PS-*b*-PDMAEMA [47] (27) (3)	63	98
Si/SiO$_2$//PS-*b*-PDMA [51] (18) (12)	42	65
Si/SiO$_2$//PS-*b*-PPFA [53] (13) (5)	112	97
Si/SiO$_2$//PS-*b*-PHFA [53] (10) (6)	127	110
Si/SiO$_2$//PS-*b*-PTFA [53] (17) (6)	101	97
Si/SiO$_2$//PS-*b*-PPFS [53] (16) (5)	121	100
Si/SiO$_2$//PS-*b*-PAA [52] (21) (8)	24	48 [c]

[a] See Table 3 for abbreviations
[b] Numbers in parentheses correspond to the individual film thickness for each block, given in nm
[c] Anisole was used as the PS-selective solvent for this system

100°. Several systems do not display this behavior (indicating little rearrangement of the diblock brush) and these correspond to blocks where $\Delta\delta > 2.6$ relative to PS. The data in Table 4 provide a better understanding of the relationship between rearrangement of diblock brushes and the relative miscibility of the two blocks. The solubility parameter is a useful predictor of brush rearrangement; the greater the difference in δ between two blocks, the less rearrangement. We have also synthesized several diblock brushes where the first block is poly(methyl acrylate) (PMA) (Table 1), but the total number of diblock systems is considerably smaller and we have excluded these systems for this discussion.

4.3
Dynamics of Surface Reorganization

To better understand the time-scale of diblock brush reorganization, we prepared semifluorinated diblock copolymer brushes where the outer block (at the air interface) was a semifluorinated block composed of poly(pentafluoro-

styrene) (PPFS), poly(heptadecafluorodecyl acrylate) (PHFA), poly(penta-fluoropropyl acrylate) (PPFA), or poly(trifluoroethyl acrylate) (PTFA) [53]. The block at the silicate interface was either PS or PMA. Treatment of the diblock systems with block-selective solvents produced predictable changes in water contact angles except for those diblock brushes based on PHFA. All of these systems were fully characterized by XPS, tensiometry, ellipsometry,
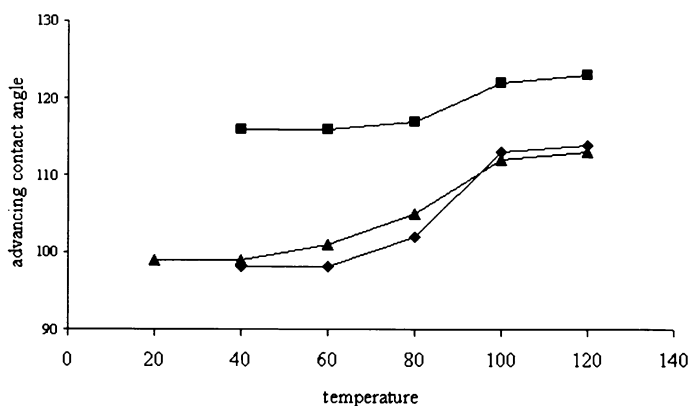

Fig. 4 Dependence of the advancing water contact angle on annealing temperature for PS-based diblock copolymer brush layers: (*filled squares*) Si/SiO$_2$//PS-*b*-PHFA, (*filled triangles*) Si/SiO$_2$//PS-*b*-PPFA, (*filled diamonds*) Si/SiO$_2$//PS-*b*-PPFS. *Lines* added as guide for the eye
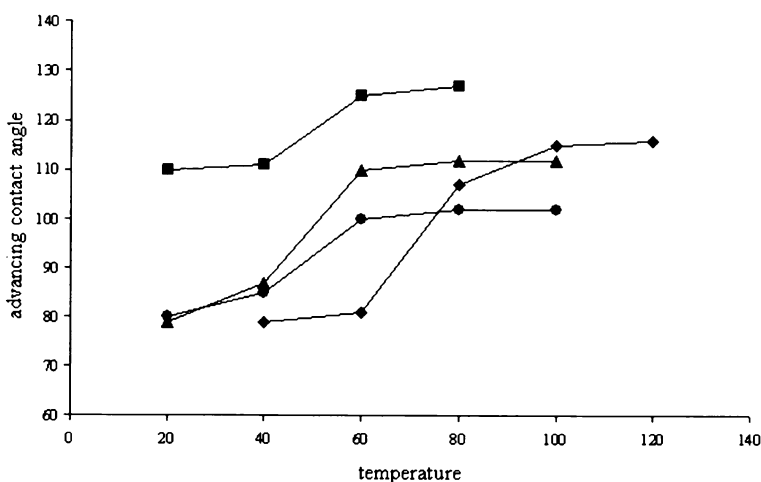

Fig. 5 Dependence of the advancing water contact angle on annealing temperature for PMA-based diblock copolymer brush layers: (*filled squares*) Si/SiO$_2$//PMA-*b*-PHFA, (*filled circles*) Si/SiO$_2$//PMA-*b*-PTFA, (*filled diamonds*) Si/SiO$_2$//PMA-*b*-PPFS, (*filled triangles*) Si/SiO$_2$//PMA-*b*-PPFA. *Lines* added as guide for the eye

AFM and ATR FTIR. Recognizing that semifluorinated blocks prefer the hydrophobic air interface, we induced a brush rearrangement of the diblock with a selective solvent for the bottom block (PS or PMA). Thermal treatment of these switched systems provided information about the time scale for equilibration to an extended state, in the absence of a solvent (see Figs. 4 and 5) [68]. Tables 5 and 6 present switching information for four out of the eight systems studied. These four diblock brushes demonstrated the greatest changes in contact angles.

Figures 4 and 5 illustrate the thermal rearrangement of semi-fluorinated diblocks after the diblock systems were treated with solvent that is selective for the lower block (PMA or PS). When either PS ($T_g = 100\,^\circ$C) or PPFS

Table 5 Solvent treatment of PS-based diblock semifluorinated brushes [a,b]

Solvent [a]	Si/SiO$_2$//PS-b-PPFS [c]		Si/SiO$_2$//PS-b-PPFA [c]	
	Θ_a	Θ_r	Θ_a	Θ_r
1st Fluorobenzene/ Trifluorotoluene [c]	121	90	112	92
1st Cyclohexane	101	85	97	78
2nd Fluorobenzene/ Trifluorotoluene [c]	119	88	113	92
2nd Cyclohexane	102	87	96	77

[a] The standard deviation of contact angles was < 2°
[b] Sample immersed in solvent at 60 °C for 1 h
[c] PS-b-PPFS brush was treated with fluorobenzene and all other brushes were treated with trifluorotoluene

Table 6 Solvent treatment of PMA-based semifluorinated diblock brushes

Solvent [a]	Si/SiO$_2$//PMA-b-PPFS [b]		Si/SiO$_2$//PMA-b-PPFA [b]	
	Θ_a	Θ_r	Θ_a	Θ_r
1st Fluorobenzene/ Trifluorotoluene [c]	115	88	111	94
1st Acetone/ Ethyl Acetate [d]	79	67	81	65
2nd Fluorobenzene/ Trifluorotoluene [c]	118	92	112	95
2nd Acetone/ Ethyl Acetate [d]	82	68	80	66

[a] Sample immersed in solvent at 60 °C for 1 h
[b] The standard deviation of contact angles was < 2°
[c] PMA-b-PPFS brush was treated with fluorobenzene and all other brushes were treated with trifluorotoluene

($T_g = 105°$) are present in the diblock brush, higher temperatures are required to effect rearrangement. Logically, the diblock brush with PMA ($T_g = 10\,°C$) and PPFA ($T_g = -\,26\,°C$) rearranges readily at lower temperatures. In addition to using heat as a switching stimulus, we have also effected the same remigration of a semifluorinated block to the air interface by subjecting a sample to supercritical CO_2. Fluoroacrylates are known to be highly soluble in supercritical CO_2 [69].

5
Summary

We have established a relationship between film thickness and the molecular weight of the polymer brush. We better understand how the relative film thickness of diblock copolymer brushes correlates with the dimensions of pinned micelle structures. Probably the most significant result is a better understanding of the relationship between rearrangement of diblock brushes and the relative miscibility of the two blocks. We have demonstrated that δ is a useful predictor of brush rearrangement; the greater the difference in between two blocks, the less significant the rearrangement. Lastly, we have demonstrated the other external stimuli besides block-selective solvents can be used to induce brush reorganization, namely temperature and treatment with supercritical CO_2.

References

1. Milner ST (1991) Science 251:905
2. Halpern A, Tirrell M, Lodge TP (1992) Adv Polym Sci 100:31
3. Zhao B, Brittain WJ (2000) Prog Polym Sci 25:677
4. Advincula RC, Brittain WJ, Caster KC, Rühe J (2004) Polymer brushes. Wiley, Weinheim
5. Mansky P, Liu Y, Huang E, Russell TP, Hawker CJ (1997) Science 275:1458
6. Delmarche E, Michel B, Biebuyck H, Gerber C (1996) Adv Mater 8:719
7. Dubois LH, Nuzzo RG (1992) Annu Rev Phys Chem 43:437
8. Matyjaszewski K (2000) In: Matyjaszewski K (ed) ACS symposium series 768. ACS, Washington, p 2
9. Prucker O, Rühe J (1998) Macromolecules 31:592
10. Prucker O, Rühe J (1998) Macromolecules 31:602
11. Wu T, Efimenko K, Genzer J (2002) J Am Chem Soc 124:9394

12. Desai SM, Solanky SS, Mandale AB, Rathore K, Singh RP (2003) Polymer 44:7645
13. Kaholek M, Lee WK, LaMattina B, Caster KC, Zauscher S (2004) Nano Lett 4:373
14. Kaholek M, Lee WK, Ahn SJ, Ma HW, Caster KC, LaMattina B, Zauscher S (2004) Chem Mater 16:3688
15. Kizhakkedathu JN, Norris-Jones R, Brooks DE (2004) Macromolecules 37:734
16. Farhan T, Huck WTS (2004) Eur Polym J 40:1599
17. Zhu X, De Graaf J, Winnik FM, Leckband D (2004) Langmuir 20:1459
18. Xu FJ, Zhong SP, Yung KYL, Kang ET, Neoh KG (2004) Biomacromolecules 5:2392
19. Zhang HJ, Ito Y (2001) Langmuir 17:8336
20. Ryan AJ, Crook CJ, Howse JR, Topham P, Jones RAL, Geoghegan M, Parnell AJ, Ruiz-Perez L, Martin SJ, Cadby A, Menelle A, Webster JRP, Gleeson AJ, Bras W (2005) Faraday Disc 128:55
21. Zhao B, Haasch RT, MacLaren S (2004) J Am Chem Soc 126:6124
22. Zhao B, He T (2003) Macromolecules 36:8599
23. Ionov L, Minko S, Stamm M, Gohy JF, Jerome R, Scholl A (2003) J Am Chem Soc 125:8302
24. Ionov L, Stamm M, Minko S, Hoffmann F, Wolff T (2004) Macromol Symp 210:229
25. Draper J, Luzinov I, Minko S, Tokarev I, Stamm M (2004) Langmuir 20:4064
26. Motornov M, Minko S, Eichhorn KJ, Nitschke M, Simon F, Stamm M (2003) Langmuir 19:8077
27. Luzinov I, Minko S, Tsukruk VV (2004) Prog Polym Sci 29:635
28. Stamm M, Minko S, Tokarev I, Fahmi A, Usov D (2004) Macromol Symp 214:73
29. Zhulina EB, Singh C, Balazs AC (1996) Macromolecules 29:6338
30. Zhulina EB, Singh C, Balazs AC (1996) Macromolecules 29:8904
31. Zhao B, Brittain WJ, Zhou W, Cheng SZD (2000) Macromolecules 33:8821
32. Zhao B, Brittain WJ, Zhou W, Cheng SZD (2000) J Am Chem Soc 122:240
33. Boyes SG, Brittain WJ, Weng X, Cheng SZD (2002) Macromolecules 35:4960
34. Huang W, Kim J-B, Baker GL, Bruening ML (2003) Nanotechnology 14:1075
35. Husseman M, Malmstrom EE, McNamara M, Mate M, Mecerreyes O, Benoit DG, Hedrick JL, Mansky P, Huang E, Russell TP, Hawker CJ (1999) Macromolecules 32:1424
36. Matyjaszewski K, Miller PJ, Shukula N, Immaraporn B, Gelman A, Luokala BB, Siclovan TM, Kickelbick G, Vllant T, Hoffmann H, Pakula T (1999) Macromolecules 32:8716
37. Zhao H, Farrell BP, Shipp DA (2004) Polymer 45:4473
38. Yu WH, Kang ET, Neoh KG, Zhu S (2003) J Phys Chem B 107:10198
39. Kong X, Kawai T, Abe J, Iyoda T (2001) Macromolecules 34:1837
40. Tomlinson MR, Genzer J (2003) Chem Comm 1350
41. Huang W, Kim J-B, Baker GL, Bruening ML (2002) Macromolecules 35:1175
42. Prokhoroava SA, Kopyshev A, Ramakrishnan A, Zhang H, Rühe J (2003) Nanotechnology 14:1098
43. Osborne VL, Jones DM, Huck WTS (2002) Chem Comm 1838
44. Quirk RP, Mathers RT, Cregger T, Foster MD (2002) Macromolecules 35:9964
45. Advincula R, Zhou Q, Park M, Wang S, Mays J, Sakellariou G, Pipas S, Hadjichristidis N (2002) Langmuir 18:8672
46. Zhao B, Brittain WJ (1999) J Am Chem Soc 121:3557
47. Zhao B, Brittain WJ (2000) Macromolecules 33:8813
48. Sedjo RA, Mirous BK, Brittain WJ (2000) Macromolecules 33:1492
49. Moineau G, Dubois P, Jerome R, Senninger T, Teyssie P (1998) Macromolecules 31:545
50. Xia J, Matyjaszewski K (1997) Macromolecules 30:7692

51. Baum M, Brittain WJ (2002) Macromolecules 35:610
52. Boyes SG, Akgun B, Brittain WJ, Foster MD (2003) Macromolecules 36:9539
53. Granville AM, Boyes SG, Akgun B, Foster MD, Brittain WJ (2004) Macromolecules 37:2790
54. Tsujii T, Ejaz M, Sato K, Goto A, Fukuda T (2001) Macromolecules 34:8872
55. Baum M (2002) PhD thesis, University of Akron
56. von Werne T, Patten TE (2001) J Am Chem Soc 123:7497
57. von Werne T, Patten TE (1999) J Am Chem Soc 121:7409
58. Schmidt R, Zhao T, Green J-B, Dyer DJ (2002) Langmuir 18:1281
59. Vaughn J, Boyes SG, Brittain WJ (2003) unpublished work
60. Ejaz M, Tsujii Y, Fukuda T (2001) Polymer 42:6811
61. Kim J-B, Bruening ML, Baker GL (2000) J Am Chem Soc 122:7616
62. Dong H, Marko JF, Witten TA (1994) Macromolecules 27:6428
63. Zhulina EB, Balazs AC (1996) Macromolecules 29:2667
64. Zhulina EB, Singh C, Balazs AC (1996) Macromolecules 29:8254
65. Gersappe D, Fasolka M, Israels R, Balazs AC (1995) Macromolecules 28:4753
66. Van Krevlen DW, Hoftyzer PJ (1976) Properties of polymers, chap 4 and 7. Elsevier, New York
67. Su W (1991) PhD thesis, The University of Akron
68. Granville AM, Boyes SG, Akgun B, Foster MD, Brittain WJ (2005) Macromolecules 38:3263
69. Behles JA, Desimone JM (2001) Pure Appl Chem 73:1281